Surface Energy and Water Budgets in the NOAA Climate Forecast System Reanalysis

Jesse Meng and the NCEP CFSR Team
Environmental Modeling Center
NCEP, NOAA, USA

Abstract

To support the mission of the National Oceanic and Atmospheric Administration (NOAA) in improving climate prediction on the seasonal scale, the National Centers for Environmental Prediction (NCEP) has produced a new generation of global reanalysis, the Climate Forecast System Reanalysis (CFSR). 31-year (1979-2009) reanalysis data set is generated as a global, high resolution, coupled atmosphere-ocean-land surface-sea ice system to provide the best estimate of the states of these coupled domains over this period. In this paper we will study the surface energy and water budgets described in CFSR. Time series of climatology means and anomalies will be analyzed including surface radiation, surface temperature, precipitation, and sea ice. Preliminary analysis has demonstrated that CFSR can advance the current understanding of the global surface energy and water cycles and their roles in the earth system to further assist the consequent research in hydrology, weather, and climate.

Key word: CFSR, Energy and Water Budgets

1. Introduction

The National Centers for Environmental Prediction (NCEP) Climate Forecast System Reanalysis (CFSR) incorporates the best available resources of fully-coupled global prediction model, in situ and satellite observations, and advanced data assimilation techniques, to make the best estimate of global climate evolution over the 31-year period of 1979-2009. The primary purpose of CFSR is to create initial conditions for historical forecasts required to calibrate the operational NCEP climate forecast. It also provides diagnoses of global climate states for researchers to assess the causes and feedbacks of climate anomalies, and to seek for further improvement in prediction skill (Saha et al., 2010).

The surface energy and water budgets, which regulate the interactions between the surface and the atmosphere, are key components in the Earth's climate system. Variables such as radiation, heat fluxes, ocean and land surface temperatures, precipitation, evaporation, and soil moisture strongly influence and influenced by the atmospheric synoptic and climate structures. Moreover, the surface energy and water budgets affect the atmosphere by determining the development of the atmospheric planetary boundary layer (Pan and Mahrt, 1987; Ek et al., 2003). Evaporation over the water surface is the primary mechanism of water transporting from the surface to the atmosphere. Contrasting to water surface, the land surface process of heat and moisture flux partitioning are much more complex with strong variability in both space and time across the climate system related to the physical properties of the surface, especially, vegetation and soil moisture content. In situ measurements of land surface energy fluxes are operated during field experiments (e.g., PILPS, Henderson-Sellers et al., 1995) and flux tower networks (e.g., FLUXNET, Baldocchi et al., 2001). However, insufficient measurement coverage in space and time makes it a challenge to assess these variables over extended period globally. A comprehensive global reanalysis serves as an alternative solution. In this paper, the structure of the surface energy and water budgets will be analyzed, focusing on the basic characteristics of several critical issues regarding climate change during the last few decades that have been widely addressed.

Corresponding author: Dr. Jesse Meng, Environmental Modeling Center, NOAA NCEP, 5200 Auth Road Suite 207, Camp Springs, Maryland 20746, USA.
E-mail: jesse.meng@noaa.gov

2. The CFSR product

The NCEP CFSR is a global fully-coupled atmosphere-ocean-land-sea ice modeling and data assimilation system. The atmospheric model used is the NCEP Global Forecast System (GFS) with horizontal resolution of 38 km globally (T382 gaussian grid) and 64 vertical levels extending from the surface to 0.26 hPa. The atmospheric data assimilation uses the NCEP Gridded Statistical Interpolation (GSI, Kleist et al., 2009). The ocean model is the Geophysical Fluid Dynamics Laboratory (GFDL) Modular Ocean Model version 4p0d (MOM4p0d, Griffies et al., 2004). The resolution is 0.25° latitude/longitude at the equator, extending to a global 0.5° beyond the tropics, with 40 levels to a depth

of 4737 m. The Global Ocean Data Assimilation System (GODAS) used is a 3DVAR assimilation scheme that has evolved from a version originally developed by Derber and Rosati (1989). The land surface model is the Noah model (Ek et al., 2003). It has 4 soil layers with fixed thickness of 10, 30, 60, and 100 cm. Within CFSR, Noah is implemented in both the fully-coupled prediction model GFS to generate the first guess fields of the land-atmosphere simulation, and in the semi-coupled global Land Information System (LIS, Peters-Lidard et al., 2007) to perform the land data assimilation (Meng et al., 2010). The sea ice model is from GFDL Sea Ice Simulator with slight modifications (Griffies et al., 2004). There are three layers in the sea ice model, including two equal layers of sea ice and one layer of snow with five categories of sea ice thickness (0-0.1, 0.1-0.3, 0.3-0.7,0.7-1.1, and a category greater than 1.1 m). Most of the variables related to surface energy and water budgets are included in the CFSR output surface flux file. CFSR provides both 6-hourly and monthly mean products. All the data used in this study is from the monthly mean product. Detail of the CFSR model and data assimilation are described in Saha et al. (2010). CFSR data is available for online access at
http://nomads.ncdc.noaa.gov/NOAAReanalysis/cfsrr

3. Results

Monthly time series of CFSR global mean surface incoming solar radiation and its climatologic anomaly are displayed in Figure 1. The variation of the global mean is dominated by a strong seasonal cycle with peaks occurring in the Southern Hemisphere summer. A notable feature in Figure 1 is the decline of peak values over the period from 2001 to 2009. The anomaly also appears to be mostly negative for the same period. The averaged flux from 2001-2009 is 191.5 Wm^{-2}, which is 1.9 Wm^{-2} below that from 1979-2000 of 193.4 Wm^{-2}.

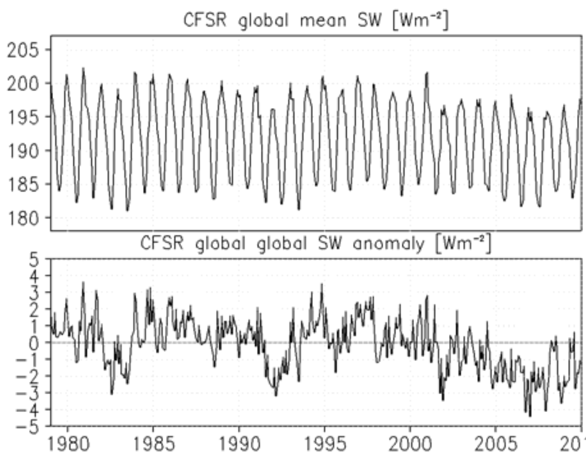

Figure 1. Monthly time series of CFSR global mean surface incoming solar radiation (top) and its anomaly (bottom).

Figure 2 shows the monthly time series of global total cloud cover percentage and its anomaly. Starting 2001, the total cloud cover increased by 2% from about 58% to above 60%. The main contribution comes from the increased tropical clouds, with the secondary contribution from the mid-latitudes of both hemispheres. While such a sustained increase in cloudiness explains the decrease in incoming solar radiation, it also influences the incoming longwave radiation at the surface (Figure 3). Owing to increased cloud emission, the surface incoming longwave radiation increased by 3.8 Wm^{-2}, from 338.9 Wm^{-2} (averaged for 1979-2000) to 342.7 Wm^{-2} (averaged for 2001-2009). Most of the contribution comes from the tropics and the mid-latitudes. Note that, for the period of 2001-2009, the increase in the incoming longwave radiation indeed surpasses the decrease in the incoming solar radiation at the surface. Therefore the net effect is increasing the total radiative energy absorbed at the surface.

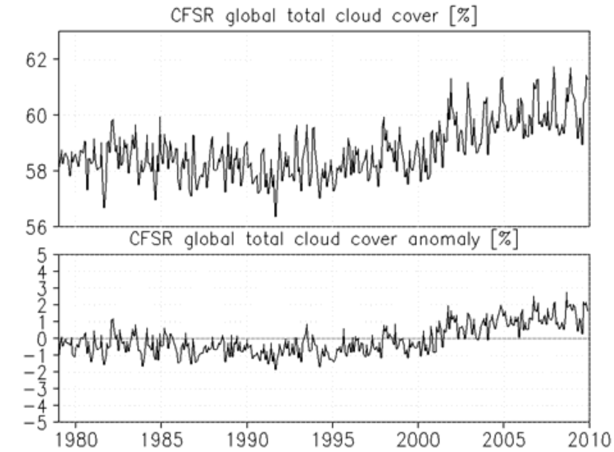

Figure 2. Monthly time series of CFSR global total cloud coverage percentage (top) and its anomaly (bottom).

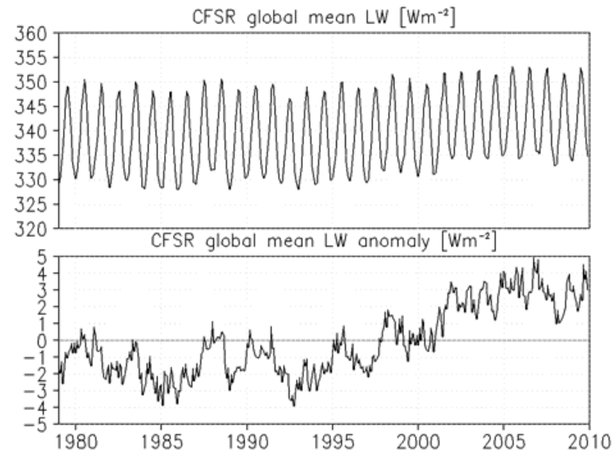

Figure 3. Monthly time series of CFSR global mean surface downward longwave radiation (top) and its anomaly (bottom).

In Figure 4, it is clear to see warm anomalies in the time series of surface air temperature for almost the entire period of 2001-2009 except for two neutral points in July 2004 and January 2008. Relatively larger warm anomaly occurs over the Northern Hemisphere land mass in this warm period. When there is more radiative energy (shortwave plus longwave) absorbed by the ocean surface, most of the energy will be consumed by evaporation and transformed back to the atmosphere in the form of latent heat flux. On the other hand, over the land surface where the available water from the soil is limited, the excessive energy is used to heat the surface and the near surface atmosphere, and transformed into terrestrial longwave radiation and sensible heat flux. The annual mean global 2 meter air temperature calculated from the CFSR data shows a warming trend of approximately 0.4 K over the 31-year period of 1979-2009. The rate becomes approximately 1.0 K over the 31 years when averaged over the land surface only.

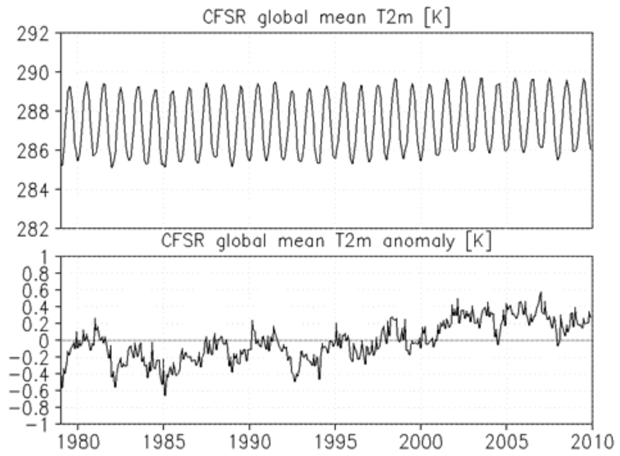

Figure 4. Monthly time series of CFSR global mean air temperature at 2 meters above the surface (top) and its anomaly (bottom).

Trends in Arctic and Antarctic sea ice cover have been highlighted as an indicator of global climate change. Serreze, et al. (2007) concluded negative trends in Arctic sea ice extent over the period of 1979-2006 in every month. The National Snow and Ice Data Center reported in a press release the Arctic sea ice cover reached the lowest level in September 2007 since satellite measurements began in 1979. Sea ice in CFSR is an assimilated field using satellite measurements hence the results are expected close to observation. Figure 5 shows the CFSR sea ice concentrations for September of 1987 (top) and 2007 (bottom) for the Arctic. It reveals a large decline of sea ice in 2007 which is consistent with previous studies. From the time series of the Arctic sea ice cover (Figure 6), large reduction is obvious for all summers of 2007, 2008, and 2009. Moreover, those three summers rank the all time lowest records over the entire CFSR period. Whereas since 2007, the annual minimum in summer has continued to recover and the wintertime extent has been about normal. On the other hand, the Antarctic sea ice cover is on a slightly positive trend since the late 1990's (not shown).

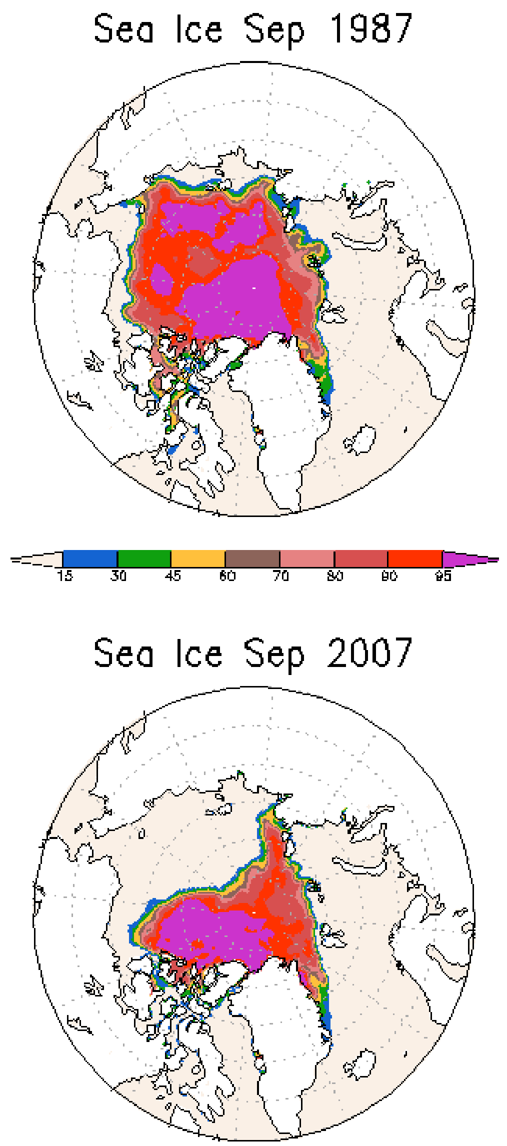

Figure 5. Maps of monthly mean Arctic sea ice concentration from CFSR for September 1987 (top) and September 2007 (bottom).

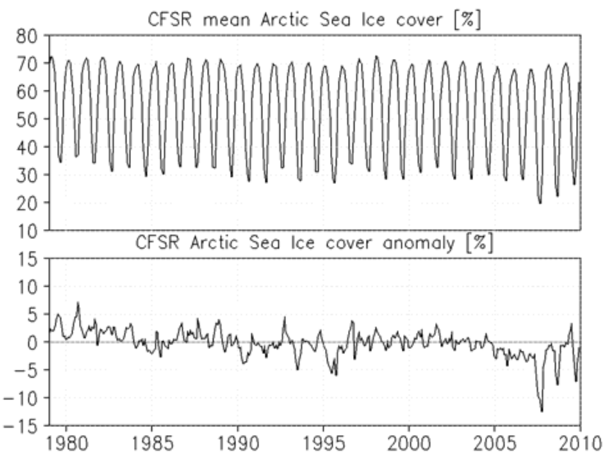

Figure 6. Monthly time series of CFSR Arctic sea ice coverage percentage (top) and its anomaly (bottom).

4. Conclusions

An updated NCEP global atmosphere-ocean-land reanalysis data set is generated for the period of 1979-2009, using improved global climate prediction and data assimilation systems. It provides an enhanced reanalysis for many aspects in climate research including assessing the global energy and water budgets. Over the 31-year period, the global surface incoming solar radiation shows a slightly downward trend due to the increasing cloudiness in the tropics and the mid-latitudes. Such a surface energy reduction is, however, compensated by an increased incoming longwave radiation from increased cloud emission. The net impact on the surface air temperature is a globally averaged 0.4 K warming over the 31-year period, or 1.0 K averaged over land surface only. Due to realistic sea ice data assimilation, the coupled CFSR has improved the analysis of sea ice concentration over the polar regions, compared to the previous reanalyses. The overall trend of sea ice cover is slightly negative for the Arctic and positive for the Antarctic, which is consistent with observations. With the lowest record occurring in September 2007, the Arctic sea ice cover reveals a tendency on track to normal for the past three years.

Acknowledgments. The authors thank Chung-Hsing Sui and Jui-Lin Li for their encouragement in conducting this study. This work is supported by the NOAA NCEP Climate Forecast System Reanalysis and Reforecast project.

References

Baldocchi, D., and co-authors, 2001: FLUXNET: A new tool to study the temporal and spatial variability of ecosystem-scale carbon dioxide, water vapor, and energy flux densities, *Bull. Aerm. Meteor. Soc*., **82**, 2415–2434.

Comiso, J. C., and F. Nishio, 2008: Trends in the sea ice cover using enhanced and compatible AMSR-E, SSM/I, and SMMR data, *J. Geophys. Res*., **113**, C02S07, doi:10.1029/2007JC004257.

Derber, J., and A. Rosati, 1989: A global oceanic data assimilation system, *J. Phys.Oceanogr.*, **19**, 1333-1347

Ek., M., K. E., Mitchell, Y Lin, E. Rogers, P. Grunmann, V. Koren, G. Gayno, and J. D. Tarpley, 2003: Implementation of Noah land-surface model advances in the NCEP operational mesoscale Eta model. *J. Geophys. Res*., **108**(D22), 8851, doi:10.1029/2002JD003296.

Griffies, S.M., M.J. Harrison, R.C. Pacanowski, and A. Rosati, 2004: Technical Guide to MOM4, GFDL *Ocean Group Technical Report No. 5*, NOAA/Geophysical Fluid Dynamics Laboratory.

Henderson-Sellers, A., A. J. pitman, P. K. Love, P. Irannejad, and T. H. Chen, The project for intercomparison of land surface parameterization schemes (PILPS), 1995: Phase 2 and 3, *Bull. Amer. Meteor. Soc*., **76**, 489-503.

Kleist, D. T., D. F. Parrish, J. C. Derber, R. Treadon, R. M. Errico, and R. Yang, 2009: Improving Incremental Balance in the GSI 3DVAR Analysis System, *Mon. Wea. Rev*., **137**, 1046-1060.

Meng, J., R. Yang, H. Wei, M. Ek, P. Xie, G. Gayno, and K. Mitchell, 2010: The land surface analysis in the NCEP Climate Forecast System Reanalysis, in preparation.

Pan, H. L., and L. Mahrt, 1987: Interaction between soil hydrology and boundary layer development, *Boundary Layer Meteorology*, **38**, 185-202.

Peters-Lidard , C.D., P.R. Houser, Y. Tian, S.V. Kumar, J. Geiger, S. Olden, L. Lighty, B. Doty, P. Dirmeyer, J. Adams, K. Mitchell, E.F. Wood and J. Sheffield, 2007: High-performance Earth system modeling with NASA/GSFC's Land Information System. *Innovations in Systems and Software Engineering*. **3**(3), 157-165. doi:10.1007/s11334-007-0028-x.

Saha, S., and co-authors, The NCEP Climate Forecast System Reanalysis, 2010: *Bull. Amer. Meteor. Soc*., in press.

Serreze, M.C., M.M. Holland, and J. Stroeve, 2007: Perspectives on the Arctic's shrinking sea-ice cover, *Science*, **315**, pp. 1533-1536, doi:10.1126/science.1139426.